Journal of the European Ceramic Society 20 (2000) 1267–1275

A TEM and HREM study of particle formation during barium titanate synthesis in aqueous solution

I. MacLaren*, C.B. Ponton

IRC in Materials for High Performance Applications and School of Metallurgy and Materials, The University of Birmingham, Birmingham B15 2TT, UK

Received 16 August 1999; received in revised form 27 October 1999; accepted 31 October 1999

Abstract

The formation mechanisms of barium titanate particles from an amorphous TiO_2 gel during synthesis in aqueous solution at temperatures between 20 and 80°C have been investigated. It was found that barium ions diffuse into the gel almost immediately, with nanocrystalline $BaTiO_3$ particles being formed after heating to just 40°C. These particles grew to dimensions of about 100 nm as the temperature was increased to 80°C, consuming the remaining TiO_2 gel. Some remnants of gel were found on particle surfaces in a sample taken at this temperature but after holding the sol at 80°C for 2 or 4 h, the particle surfaces became "cleaner" and more rounded. It is proposed on the basis of these observations that the $BaTiO_3$ particles were formed by an in-situ transformation of the amorphous TiO_2 gel. The mechanism by which (i) the particles were then rounded off and (ii) the final gel fragments were incorporated into the main $BaTiO_3$ particles was, however, less clear. © 2000 Elsevier Science Ltd. All rights reserved.

Keywords: $BaTiO_3$ and titanates; Electron microscopy; Powders-chemical preparation

1. Introduction

Barium titanate ($BaTiO_3$) is used widely in the electronics industry, especially in multilayer capacitors due to its high dielectric constant. It is produced conventionally by the solid-state reaction of $BaCO_3$ with TiO_2 at temperatures above 900°C. This method, however, leads to the production of large $BaTiO_3$ particles with uncontrolled and irregular morphologies, which can limit the electrical properties of the resulting sintered ceramics.

By contrast, hydrothermal synthesis has been shown to be a viable route for the production of barium titanate and can be used to produce fine (< 1 μm) or ultrafine ($<$ 100 nm) particles with a controlled, rounded morphology, a narrow size distribution, and of high purity. Such particles are very well suited for use in modern green fabrication techniques such as tape casting, inkjet printing, etc. Furthermore, they sinter well at temperatures lower than those used to sinter conventionally produced powders (up to 200°C lower in some cases). This allows the grain size of the resulting ceramic to be tailored to the optimum value for the desired electrical properties by control of the sintering schedule and hence degree of grain growth. For these reasons, the hydrothermal production of barium titanate has been commercialised in both the United States and Japan, with the resultant powders finding niche applications.

There have been many investigations concerning the hydrothermal synthesis of barium titanate (for example Refs. 1–7), generally focussing on a variety of aspects, such as: structural, microstructural, and chemical characterisation; doping with other elements during the hydrothermal synthesis process; and the sintering behaviour of green bodies made from hydrothermally produced barium titanate. It is only more recently, however, that attempts have been made to understand the mechanism(s) by which the barium titanate particles are formed during hydrothermal processing.

Hertl[8] used the kinetic analysis of reaction rates in an attempt to understand the reaction mechanisms leading to the formation of barium titanate from TiO_2 powder suspended in $Ba(OH)_2$ solution. He assumed that the barium titanate is formed on the surface of the TiO_2 particles by an in-situ transformation of the TiO_2 as Ba

* Corresponding author at present address: Department of Experimental Physics, Chalmers University of Technology, S-41296 Göteborg, Sweden. Tel.: +46-31-772-3633; fax: +46-31-772-3224.

E-mail address: maclaren@fy.chalmers.se (I. MacLaren).

0955-2219/00/$ - see front matter © 2000 Elsevier Science Ltd. All rights reserved.
PII: S0955-2219(99)00287-3

ions diffuse into the structure. Chien et al.[5] investigated the microstructural evolution of $BaTiO_3$ as it formed from TiO_2 particles in $Ba(OH)_2$ solution. It was shown that small particles of $BaTiO_3$ form initially on the surfaces of the TiO_2 particles, with all the TiO_2 particles being converted eventually to $BaTiO_3$ particles having a raspberry-like appearance, and that further hydrothermal treatment results in smoothing of the $BaTiO_3$ particle surfaces to form rounded particles. Eckert et al.[9] combined thermodynamic modelling, TEM microstructural characterisation, and the kinetic analysis of reaction rates. Similar conclusions to Chien et al.[5] were reached concerning the microstructural evolution of $BaTiO_3$ particles. Reaction rate analysis seemed to indicate that the early stages were dominated by a dissolution–precipitation mechanism in contrast to the earlier work by Hertl,[8] in which it was claimed that an in-situ transformation mechanism was responsible. The mechanism operating in the later stages of the reaction was, however, less clear. Kerchner et al.[10] also used reaction rate analysis and TEM characterisation of the particles, reaching similar conclusions. It appears, however, from the TEM observations of Chien et al.[5] and Eckert et al.,[9] that the $BaTiO_3$ particles form initially as very small particles just a few nanometres in size, which tend to cluster together. After continued hydrothermal processing, these clustered particles appear to end up as larger, single crystal $BaTiO_3$ particles.

Aksay et al.[11] shed further light on the transformation mechanism. They placed $BaTiO_3$ seed particles in a suspension of TiO_2 particles in aqueous $Ba(OH)_2$, and after a short hydrothermal treatment, collected particles on a grid for HREM observation. It was found that newly formed $BaTiO_3$ nuclei became attached to the seed particles and that the small nuclei tended to rotate into the same orientation as the larger seed particle. It was inferred from this that the nuclei are produced by homogeneous nucleation in solution at the high reactant concentrations typically used in hydrothermal synthesis which then tended to agglomerate due to van der Waals and/or electrostatic attraction forces. This effect could also result in the raspberry-like particle morphologies observed by Chien et al.[5] and Eckert et al.[9] These observations appear to support the dissolution–precipitation model proposed by Eckert et al.[9] for the early stages of particle formation.

Not all hydrothermally synthesised $BaTiO_3$ is, however, made from crystalline TiO_2. It is frequently produced from hydrous titanium oxide gels produced by the hydrolysis of compounds such as $TiCl_4$ or Ti alkoxides with water. It is commonly recognised that these Ti-containing gels are more reactive than crystalline TiO_2, and hence, that the reaction rate for the formation of $BaTiO_3$ is much faster than when TiO_2 is used. Moreover, it is likely that the reaction mechanism differs from that for the formation of barium titanate from crystalline TiO_2. Kerchner et al.[11] analysed the synthesis of $BaTiO_3$ from hydrous TiO_2 gels, employing both reaction rate analysis and TEM characterisation of the particles. They concluded from the reaction rate analysis that the reaction probably proceeds by "a phase boundary controlled mechanism where the initial crystallisation is controlled by an interfacial chemical reaction". From some of their TEM observations, however, they contradicted this by stating that the homogeneous, uncored structure of the small crystallites possibly implies a dissolution–precipitation type mechanism. They concluded finally, that the reaction probably proceeds by Ba^{2+} ions infiltrating the hydrous TiO_2 gel and reacting at the surfaces to form $BaTiO_3$.

In this paper we report on an investigation of the formation mechanisms of $BaTiO_3$ particles produced from a hydrous TiO_2 gel. Conventional TEM with Energy Dispersive X-ray analysis was used to determine the general morphology of particles and the Ba/Ti ratio, and HREM to investigate the structure of crystallites at a much finer scale.

2. Experimental procedure

The raw materials used were barium acetate, $Ba(CH_3COO)_2$ (Aldrich Chemical Co., Gillingham, Dorset), titanium isopropoxide, $Ti(OC_2H_4CH_3)_4$, (Tilcom TIPT), and the organic base, tetramethylammonium hydroxide $[(CH_3)_4NOH]$, (Aldrich Chemical Co., Gillingham, Dorset). Alkaline conditions were used since all previous work on the hydrothermal synthesis of barium titanate has shown such conditions to be necessary for the formation of the perovskite phase.

Quantities of precursors were chosen such that they would produce a concentration of 0.25 mol l^{-1} of $BaTiO_3$ in suspension if the precursors reacted to completion. The amount of tetramethylammonium hydroxide was chosen such that it would give a ratio of OH^- to total metal ions of 2:1. In view of the fact that a small amount of barium ions is often found to remain in solution during the hydrothermal synthesis of barium titanate, 2 mol% more barium acetate was used than would be necessary to achieve stoichiometry. A sol was made by dissolving the barium acetate in the appropriate quantity of water, adding the tetramethylammonium hydroxide solution while stirring, followed by the titanium isopropoxide. The titanium isopropoxide is hydrolysed on contact with the aqueous solution to form an amorphous polymeric titanium oxide gel.[12] After 5 min of stirring, the pH and temperature were measured, and a small sample extracted by pipette. The sol was then heated in an open topped PTFE-lined autoclave (Berghof GmbH, Germany) to 80°C over a period of about 30 min, during which time the pH was measured and small samples taken at 40, 60, and 80°C.

The sol was then kept at 80°C for 4 h, with the pH again being measured and small samples extracted by pipette after 2 h and finally after 4 h. Each of these samples was transferred to a small specimen tube containing water to dilute it and disperse the sol particles. A copper grid with a supported thin carbon film was dipped into the diluted sol, removed, and then allowed to dry on filter paper, resulting in a dispersion of the small sol particles on the carbon film.

The particles on the supported carbon films were then examined using: a JEOL 200CX HR-TEM to investigate their morphology and crystalline structure; a JEOL 4000FX TEM equipped with a LINK AN10000 EDX system with a Si(Li) detector (nominal resolution 162 keV at Mn K_α) to do conventional bright field imaging and to analyse the chemical composition of the particles; and a Philips CM20 TEM to do conventional bright field imaging. All the microscopes were equipped with LaB_6 electron sources.

The JEOL 200CX was equipped with a top-entry stage and had a point-to-point resolution of about 2.4 Å. Since no specimen height adjustment is provided, the exact position in the objective lens varies slightly from one specimen to another giving slightly different magnifications than the quoted magnification. Nevertheless, for a typical specimen, the magnification should be within ±10% of the quoted value, and thus the nm scale markers on the micrographs should be accurate to within ±10%.

EDX quantification of Ba:Ti ratios is problematic because of the overlap between the K_α and K_β peaks for Ti at 4.508 and 4.931 keV, respectively, and the largest two L peaks for Ba (Lα and $L\beta_1$), at 4.465 and 4.827 keV, respectively. Whilst problematic, it is not impossible because Ba has other less intense L peaks for which Ti has no counterpart including the $L\beta_2$ peak at 5.156 keV and the $L_{\gamma 1}$ and $L_{\gamma 2}$ peaks at slightly higher energies. The quantification was performed using the RTS-2/FLS software on the LINK AN10000 system using the theoretical k-factors provided, and experimentally acquired profiles for Ba and Ti.

In view of these quantification difficulties, it is thought that the accuracy of quantification is unlikely to be as good as for systems where the peaks are well separated; therefore, the absolute accuracy would certainly not be better than ±5 at%. Having said this, the reproducibility of results on a particular type of particle was usually very good (usually better than ±3 at%) suggesting that quantification is reliable. The errors quoted on averages of several quantified EDX results merely represent the standard deviation of the different results (i.e. the reproducibility) and do not include any estimate of the deviation from absolute accuracy, i.e. the precision rather than the accuracy of the experimental results is given. All quantified EDX results are quoted in atomic % of Ba and Ti; oxygen was not quantified since it was difficult to obtain reliable results.

3. Results

As stated above, samples were taken at various stages during hydrothermal processing so that the development of the $BaTiO_3$ particles could be monitored. The temperature and pH values of the sol at each sampling point are recorded in Table 1 below. It can be seen that the pH stayed above 12 for the entire duration of the reaction. It may have been expected that the pH would have been reduced as the reaction proceeded to completion, due to neutralisation of the organic base by the acetate ions formed as a by-product of the reaction that forms barium titanate:

$$Ba(CH_3COO)_2\,(aq) + TiO_2.xH_2O\,(s) + 2(CH_3)_4NOH\,(aq) \Rightarrow BaTiO_3\,(s) + 2(CH_3)_4N^+CH_3COO^-\,(aq) + (1+x)H_2O\,(l) \quad (1)$$

Instead of this, the readings show an increase in pH with increasing reaction temperature. This apparent increase in pH with increasing reaction temperature could, however, be a result of insufficient temperature compensation on the pH meter used to take these readings (since the pH meter employed did have a temperature compensation feature). It may be, however, that part of the pH rise was real, perhaps as a result of increased dissociation of the organic base, TMAH, at the higher temperatures.

All samples contained barium-rich needle shaped particles. These were believed to be barium acetate powder particles that had not fully dissolved, or had reformed on drying of the diluted sol on the copper grid. All the samples contained some $BaCO_3$ particles, probably formed by the dissolution of atmospheric CO_2 in the alkaline solution, followed by the precipitation of insoluble $BaCO_3$. The production of $BaCO_3$ impurities is normal in the hydrothermal synthesis of $BaTiO_3$ unless great care is taken to ensure that the precursors and the reaction environment are CO_2-free. These barium acetate and barium carbonate particles are not, however, considered further in this text, as they were thought not to affect the growth mechanisms of the $BaTiO_3$ particles.

Table 1
Temperature and pH of the sol at the taking of each sample

Sample number	Temperature (°C)	pH
1	25	12.05
2	40	12.23
3	60	12.37
4	80	12.8
5	80 for 2 h	13.0
6	80 for 4 h	12.8

3.1. Sample 1 (25°C)

This sample consisted mainly of amorphous gel. Fig. 1a shows a conventional bright field TEM micrograph of a typical region of gel with a SAD pattern inset. As in the case of the gel used by Kerchner et al.,[10] it is highly porous, containing many small channels which would give it a very high surface area in contact with the hydrothermal solution. EDX analysis of the gel shows that it is strongly Ti-rich but it does contain some Ba ions as well: an average of several analyses gives a composition of 83 ± 3 at% Ti, 17 ± 3 at% Ba.

Fig. 1b shows an HREM image of an area of gel adjacent to a small hole, this clearly shows the amorphous structure of both the gel and the carbon film support (lower left). No evidence of any crystallinity was found in the gel from this sample.

3.2. Sample 2 (40°C)

This sample comprises mainly the hydrous TiO_2 gel and Fig. 2a shows a micrograph of a typical area with a SAD pattern inset. This diffraction pattern shows only faint diffuse rings indicative of amorphous material; although some other SAD patterns from this sample also show faint, diffuse diffraction spots, suggesting that there may be incipient crystallisation of the gel. These faint spots appear at positions that could be consistent with plane spacings for $BaTiO_3$. EDX analysis of a number of areas yielded an average composition of 77 ± 3 at% Ti, 23 ± 3 at% Ba. A number of areas had some particles with sizes >10 nm that were noticeably more crystalline.

Fig. 2b is an HREM image of one area of gel which appeared amorphous from lower magnification TEM and SAD. This image shows many very small crystallites with dimensions of only a few nanometres forming in the gel; some of these crystallites are indicated with arrows. Such nanometre scale crystallites were found in many apparently non-crystalline regions of gel. The fringe spacings are consistent with those that would be expected for cubic $BaTiO_3$. This confirms that these particles are small crystalline nuclei of $BaTiO_3$.

3.3. Sample 3 (60°C)

Fig. 3a shows a bright field image of a typical gel area in this sample with a SAD pattern inset. It may be noted that a number of discrete crystalline particles with sizes of up to 100 nm have formed in the amorphous gel. SAD patterns from such regions show discrete diffraction spots originating from these particles, as well as amorphous rings originating from the gel; the d-spacings for the spots are consistent with the perovskite $BaTiO_3$ structure. EDX analyses of the gel showed results which varied widely from one position to another; an average of five analyses gave a composition of 73 ± 7% Ti, 27 ± 7% Ba. The barium titanate particles in the gel had near-stoichiometric compositions of 49 ± 3 at% Ti, 51 ± 3 at% Ba.

Fig. 3b shows an HREM image of the edge of one of these $BaTiO_3$ particles growing in the gel. It may be seen that the particle, whilst having continuous fringes (implying that it is a single crystal), seems to have formed through the coalescence of several smaller particles. Some crystallites with different orientations are observed at the edges (indicated with arrows). It is likely, therefore, that several small crystallites like those in Fig. 2b have merged to form one larger single crystal

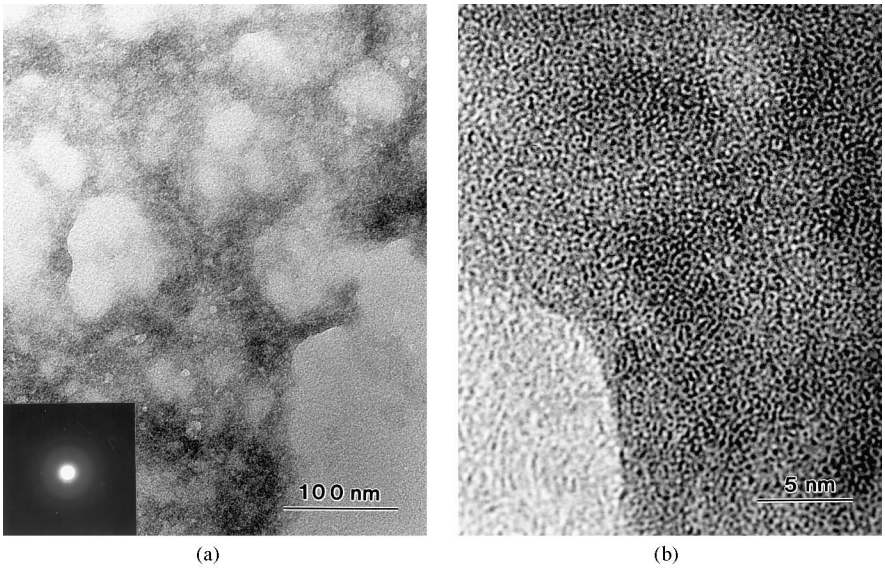

(a) (b)

Fig. 1. Micrographs of TiO_2 gel from sample 1 (extracted at 25°C): (a) bright field TEM image with SAD pattern inset; (b) HREM image of an area adjacent to a small hole.

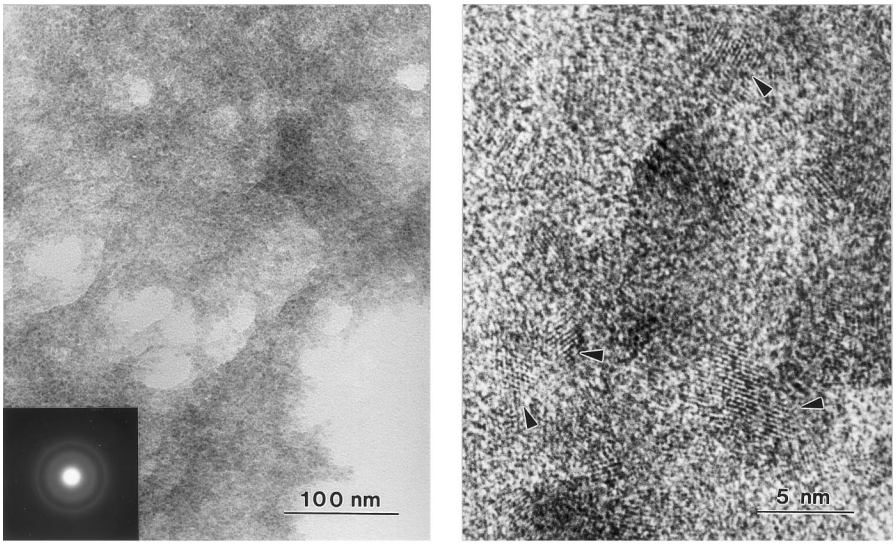

Fig. 2. Micrographs of TiO_2 gel from sample 2 (extracted at 40°C): (a) bright field TEM image with SAD pattern inset; (b) HREM image showing the formation of small crystallites (arrowed).

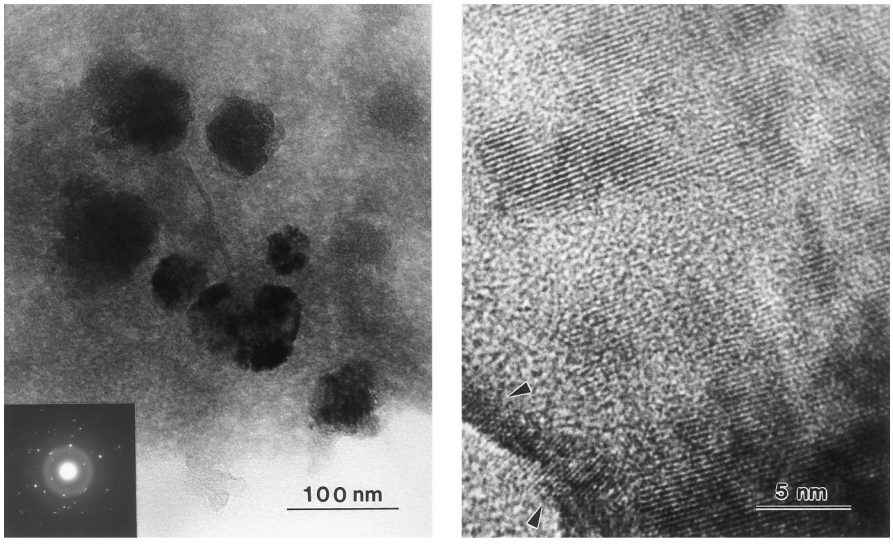

Fig. 3. Micrographs of TiO_2 gel containing $BaTiO_3$ particles from sample 3 (extracted at 60°C): (a) bright field TEM image with SAD pattern inset; (b) HREM image showing the edge of one $BaTiO_3$ crystal embedded in gel, two nanosized crystallites are arrowed.

particle but others were still separate from the main large $BaTiO_3$ particle at the time of sampling.

3.4. Sample 4 (80°C)

The particles in this sample were quite different from those in previous samples, with very little gel being visible. Fig. 4a is a TEM micrograph of some typical particles in this sample, with a SAD pattern of these particles inset. Most particles are rounded single crystal particles with dimensions in the range 80–120 nm. Some particles consist of several crystals separated by grain boundaries; the three particles indicated by arrows consist of at least three crystals each. The SAD pattern is clearly consistent with these being $BaTiO_3$ particles, while EDX analyses of several particles gave an average composition of 47 ± 3 at% Ti, 53 ± 3 at% Ba, which is close to stoichiometry. The particle size is variable, however, and the particles are somewhat "knobbly" around the edges.

Fig. 4b is an HREM micrograph of the edge of one $BaTiO_3$ particle. The {110} lattice fringes of the $BaTiO_3$

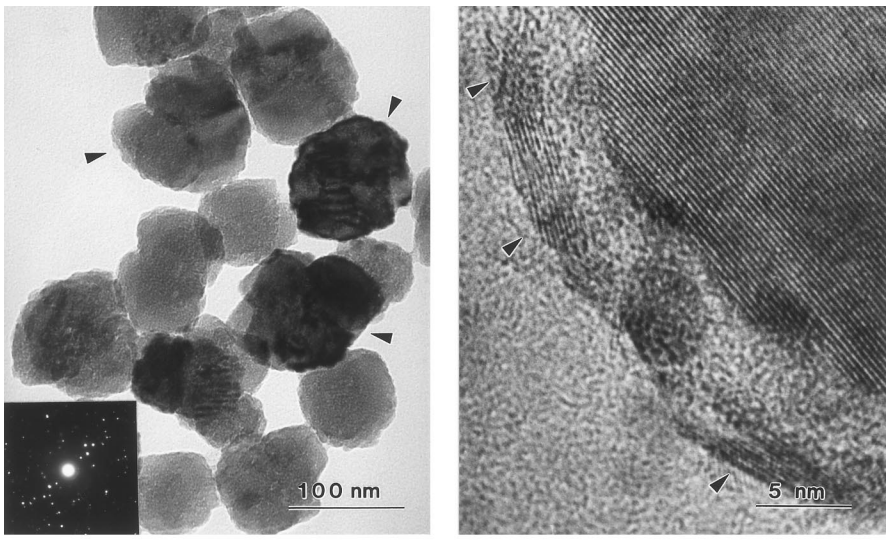

(a) (b)

Fig. 4. Micrographs of $BaTiO_3$ particles from sample 4 (extracted at 80°C): (a) bright field TEM image with SAD pattern inset, three particles each consisting of at least three crystallites are arrowed; (b) HREM image showing the edge of a $BaTiO_3$ crystal, some nanoscale crystallites at the edge of the particle are indicated with arrows.

are clearly visible but around the edge of the particle there is a mostly amorphous region which is approximately 5 nm thick. There are also crystalline regions in this outer layer, displaying lattice fringes as indicated by arrows. Such an observation has been made on a number of particles from this sample. It seems that while most of the particles in this sample had become separated from the amorphous TiO_2 gel, many still had some remnants of this gel as a thin layer around the edges.

3.5. Sample 5 (80°C/2 h)

The particles of this sample were fairly similar to those of the previous sample. Fig. 5a is a TEM image of one group of particles in this powder with a SAD pattern inset. As before, the SAD pattern is consistent with the particles being of the $BaTiO_3$ phase. The average composition of several groups of particles was 48 ± 3 at% Ti, 52 ± 3 at% Ba; which is close to that for the previous sample.

Fig. 5b is an HREM image of the edge of one particle from this powder. The {111} lattice fringes for $BaTiO_3$ are clearly visible but there is a clear difference from Fig. 4b in that the edge of the particle is much "cleaner". In general, very few particles were found to have traces of remnant gel on their edges.

3.6. Sample 6 (80°C/4 h)

The particles of this sample were again fairly similar in size and morphology to those of the previous two samples. A typical group of such particles is shown in Fig. 6a with a SAD pattern inset. It may be observed that the edges of particles are in general more rounded and less "lumpy" or angular than those in samples 4 and 5. The SAD pattern is once again consistent with the $BaTiO_3$ structure. The average composition for several groups of particles is 47 ± 2 at% Ti, 53 ± 2 at% Ba, which is near-stoichiometric and similar to that for the previous two particles.

An HREM image of the edge of one particle is shown in Fig. 6b. This particle is oriented close to the ⟨001⟩ axis with the fringes for the two perpendicular sets of {100} planes showing clearly. Again, it may be seen that the edge is clean and free of any remnant gel. No particles were found which showed any remnants of gel on the edges.

4. Discussion and proposed particle formation mechanism

Although small crystallites of $BaTiO_3$ formed in TiO_2 gels have previously been observed in the early stages of hydrothermal synthesis,[10] no EDX analyses of the gels were conducted and no definite conclusion was drawn as to whether they were formed by an in-situ transformation mechanism or by a dissolution–precipitation mechanism. Thus, the EDX results from this study shed further light on the particle formation mechanism(s).

It appears that, prior to the crystallisation of $BaTiO_3$, Ba^{2+} ions had diffused into the gel to a significant degree (at least 15–20 at% at 25°C); although, it may be that these were mainly adsorbed onto external surfaces at first, as suggested by Hennings et al.[2] The first nanoscale crystallites then appeared at a temperature of just 40°C, when the gel had a composition of about 20–25 at% Ba. Thus, it seems clear that an in-situ transformation of the gel was occurring, probably starting at

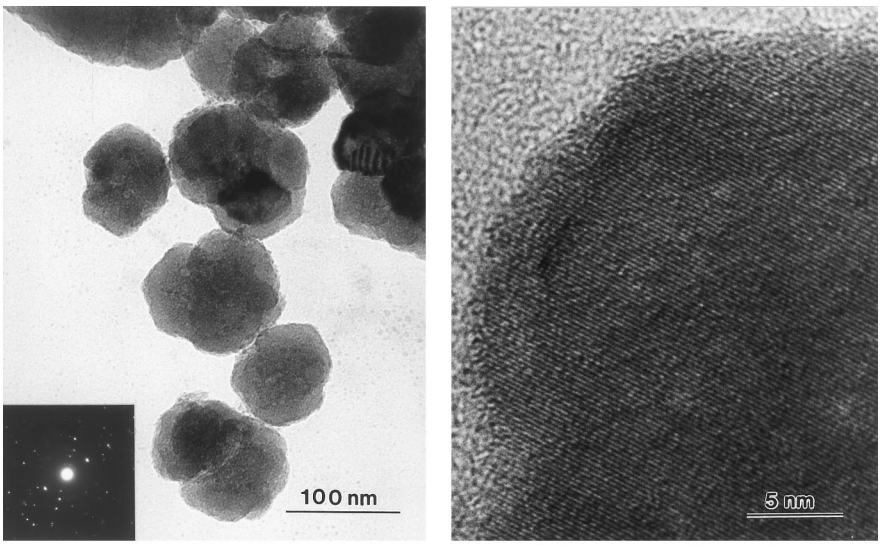

Fig. 5. Micrographs of $BaTiO_3$ particles from sample 5 (extracted after 2 h treatment at 80°C): (a) bright field TEM image with SAD pattern inset; (b) HREM image showing the edge of a $BaTiO_3$ crystal.

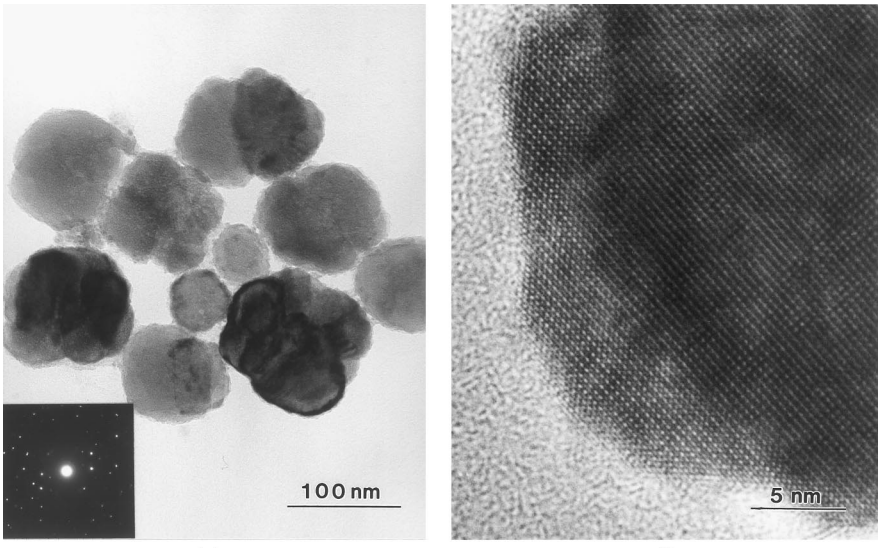

Fig. 6. Micrographs of $BaTiO_3$ particles from sample 6 (extracted after 4 h treatment at 80°C): (a) bright field TEM image with SAD pattern inset; (b) HREM image showing the edge of a $BaTiO_3$ crystal.

the surfaces, as finally considered by Kerchner et al.,[10] resulting in the formation of these nanoscale crystallites. It is interesting to note that previously the first nucleation of $BaTiO_3$ had been noted by other workers only at higher temperatures $\geqslant$ 70°C. These nanoscale crystallites grew further into the gel and started to grow into one another as the temperature was increased to 60°C. In the majority of cases, it appeared that the nanoscale crystallites had coalesced into larger single crystals with any grain boundaries being eliminated, although the mechanism by which the boundaries are eliminated is not at all clear. It seems unlikely that it could happen by crystallite rotation since most crystallites are constrained by the surrounding gel, a more likely mechanism being boundary migration. These crystalline particles were found to have compositions close to that for stoichiometric $BaTiO_3$.

As the gel was consumed and transformed into $BaTiO_3$ crystals on increasing the temperature to 80°C, the resulting crystals became separated from the gel, and were usually found as small clusters, probably held together by van der Waals and/or electrostatic attraction forces. After initially heating to 80°C, some remnants of the gel were still found on the edges of particles

in the form of amorphous material and nanoscale $BaTiO_3$ crystallites. After prolonged treatment at 80°C, however, the particles were found to have "cleaner" edges and had become more rounded, although the particle size was not changed significantly. This suggests that any remaining gel remnants were incorporated into the $BaTiO_3$ crystallites, possibly by rotation or by boundary migration of any small crystallites, along with crystallisation of the remaining amorphous gel. The mechanism by which protrusions, bumps and sharp edges are rounded is uncertain. It could well be that this occurs by dissolution–precipitation, since such features would display higher local solubility than other areas of particle surfaces due to the high degree of surface curvature, resulting in preferential dissolution of such features and re-precipitation on other less curved areas of particles. Regardless of whether this is the case or not, it is clear that this process proceeds by a totally different mechanism to the initial particle formation, since the nature of the particles changed markedly from that during the early phases of synthesis, and because the subsequent reaction rate was much slower than that during the initial particle formation stage.

All the work in this study was carried out at $\leqslant 80$°C in an open system under atmospheric pressure, and so it could be argued that the reaction mechanisms that operate during hydrothermal synthesis in a closed pressure vessel at higher temperatures and pressures would be somewhat different from this. The initial nucleation and growth of $BaTiO_3$ particles from within the gel were, however, found to occur at very low temperatures of less than 60°C. Table 2 shows the vapour pressures for water at the sampling temperatures used in this study.[13] It can be seen clearly that the vapour pressure only starts to increase appreciably at 60°C and above; thus, the autogeneous pressure in a sealed vessel is not likely to differ greatly from atmospheric pressure until temperatures above 60°C are achieved. Even then, the vapour pressure at 80°C is still less than 0.5 bar and such a small pressure difference is unlikely to make a significant difference to the chemical processes occurring in solution. It may also be noted that some of the early work on the "hydrothermal" synthesis of $BaTiO_3$ was carried out in an open beaker at 90–100°C.[14]

In contrast to this, the mechanism by which the surfaces of the $BaTiO_3$ particles are smoothed and rounded may vary with hydrothermal processing temperature and pressure, and it is almost certain that the reaction rate for this process will be strongly dependent upon temperature.

Table 2
Vapour pressure of water at various temperatures (after Weast[13])

Temperature (°C)	Vapour pressure (bar)
25	0.371
40	0.073
60	0.197
80	0.467

5. Summary

The mechanisms for the formation of $BaTiO_3$ particles have been investigated for the synthesis of $BaTiO_3$ from a hydrous TiO_2 gel formed from the in-situ hydrolysation of titanium isopropoxide in a solution of barium acetate and the strong organic base, tetramethylammonium hydroxide in an open system under atmospheric pressure.

It was found that Ba ions diffused into the gel at 25°C, resulting in the formation of nanoscale crystallites of $BaTiO_3$ in the gel after heating the reaction mixture to 40°C. These crystallites grew within and into the gel on continued heating to 60°C, forming larger crystals with dimensions of about 50–100 nm. Further heating to 80°C resulted in the consumption of most of the remaining gel, leaving clusters of $BaTiO_3$ particles which had slightly bumpy surfaces and dimensions of the order of 100 nm. Many of these particles still retained some remnants of the gel as a surface layer which was a few nanometres thick. Further treatment at 80°C for 2 and 4 h resulted in the elimination of this layer and the rounding of particle surfaces.

It is proposed on the basis of these observations that the initial nucleation and growth of the particles proceeded by in-situ transformation, while the mechanism for the rounding of particles is less clear but is most likely a dissolution–precipitation type mechanism.

Acknowledgements

The authors would like to thank Professor M.H. Loretto (Director of the IRC in Materials for High Performance Applications) and Professor I.R. Harris (Head of the School of Metallurgy and Materials) for the provision of laboratory facilities. Financial support for this work was provided by the Engineering and Physical Sciences Research Council.

References

1. Vivekanandan, R., Philip, S. and Kutty, T. R. N., Hydrothermal preparation of $Ba(Ti,Zr)O_3$ fine powders. *Mater. Res. Bull.*, 1986, **22**, 99–108.
2. Hennings, D., Rosenstein, G. and Schreinemacher, H., Hydrothermal preparation of barium titanate from barium–titanium acetate gel precursors. *J. Eur. Ceram. Soc.*, 1991, **8**, 107–115.
3. Dutta, R. K. and Gregg, J. R., Hydrothermal synthesis of tetragonal barium titanate. *Chem. Mater.*, 1992, **4**, 843–846.
4. Menashi, J., Reid, R. C. and Wagner, L. P., Barium titanate based dielectric compositions. US patent 4832939, 1989.

5. Chien, A. T., Speck, L. S., Lange, F. F., Daykin, A. C. and Levi, C. G., Low temperature/low pressure hydrothermal synthesis of barium titanate: powder and heteroepitaxial thin films. *J. Mater. Res*., 1995, **10**, 1784–1789.
6. Xia, C. T., Shi, E. W., Zhong, W. Z. and Guo, J. K., Preparation of $BaTiO_3$ by the hydrothermal method. *J. Eur. Ceram. Soc*., 1995, **15**, 1171–1176.
7. MacLaren, L., Ponton, C. B., Elgy, C. N. and Knott P. R., The effects of synthesis temperature upon hydrothermally produced $BaTiO_3$ powders. In *Proceedings of Electroceramics V*, Vol. 2, ed. J. L. Baptista, J. A. Labrincha and P. M. Vilarinho. European Ceramic Society, 1996, pp. 375–378.
8. Herd, W., Kinetics of barium titanate synthesis. *J. Am. Ceram. Soc*., 1988, **71**, 879–883.
9. Eckert Jr., J. O., Hung-Houston, C. C., Gersten, B. L., Lericka, M. M. and Riman, R. E., Kinetics and mechanisms of hydrothermal synthesis of barium titanate. *J. Am. Ceram. Soc*., 1996, **79**, 2929–2939.
10. Kerchner, J. A., Moon, J., Chodelka, R. E., Morrone, A. and Adair, J. H., Nucleation and formation mechanisms of hydrothermally derived barium titanate. ACS Symposium Series, Vol. 681. American Chemical Society, 1998, pp. 106–119.
11. Aksay, I. A., Chun, C. M. and Lee, T., Mechanisms of $BaTiO_3$ formation by hydrothermal reactions. In *Proceedings of The Second International Conference on Solvothermal Reactions*, Takamatsu, Japan, 1996, pp. 76–79.
12. Tioxide Chemicals, Safety Data Sheet. Tilcom TIPT, circa 1992.
13. Weast, R. C. (ed.), *CRC Handbook of Chemistry and Physics*. CRC Press, Cleveland, OH, 1980, p. D-159.
14. Kiss, K., Magder, J., Vukasovich, M. S. and Lockhart, R. J., Ferroelectrics of ultrafine particle size: I, synthesis of titanate powders of ultrafine particle size. *J. Am. Ceram. Soc*., 1966, **49**, 291–293.